Princeton Plasma Physics Laboratory

PPPL- 4287

PPPL- 4287

The Linear Stability Properties of Medium- to High- n TAEs in ITER

N. N. Gorelenkov, H. L. Berk, R. V. Budny, C.E. Kessel,
G.J. Kramer, D. McCune, J. Manickam, R. Nazikian and A. Polevoi

February 2008

PPPL
PRINCETON PLASMA
PHYSICS LABORATORY

Prepared for the U.S. Department of Energy under Contract DE-AC02-76CH03073.

Princeton Plasma Physics Laboratory
Report Disclaimers

Full Legal Disclaimer

Trademark Disclaimer

PPPL Report Availability

Princeton Plasma Physics Laboratory:

http://www.pppl.gov/techreports.cfm

Office of Scientific and Technical Information (OSTI):

http://www.osti.gov/bridge

Related Links:

U.S. Department of Energy

Office of Scientific and Technical Information

Fusion Links

The linear stability properties of medium- to high- n TAEs in ITER

N. N. Gorelenkov[1], H. L. Berk[2], R. V. Budny[1], C.E. Kessel[1], G.J. Kramer[1], D. McCune[1], J. Manickam[1], R. Nazikian[1], A. Polevoi[3]
[1]Princeton Plasma Physics Laboratory, Princeton University
[2]Institute for Fusion Studies, Unviersity of Texas, Austin
[3]ITER team & Kurchatov Institute, Moscow*

Executive summary

This document provides a detailed report on the successful completion of the DOE OFES Theory Milestone for FY2007: *Improve the simulation resolution of linear stability properties of Toroidal Alfvén Eigenmodes (TAE) driven by energetic particles and neutral beams in ITER by increasing the numbers of toroidal modes used to 15.*

In the course of the performed systematic study, equilibria representing the evolution of thirteen distinct plasma conditions were developed and analyzed to investigate the Alfvén Eigenmode stability. The Tokamak Start-up Code, TSC [1], and the plasma transport simulation code, TRANSP [2], were used to develop three fiducial equilibria for the three main ITER scenarios: the elmy H-mode, hybrid and advanced (AT or reversed shear) plasma regimes. The simulations addressed the evolution from start-up to steady-state for a period of a thousand seconds. TSC was used to simulate the start-up and control of the plasma boundary, and TRANSP was used to obtain accurate particle distribution functions for the slowing down negative neutral beam injected (NNBI) ions, as well as the thermonuclear alpha-particles. In addition to the three fiducial ITER scenarios, ten additional plasmas, with varying NNBI injection angle and current drive schemes, were developed for the elmy H-mode, hybrid, and AT scenarios. This enables an evaluation of the potential of controlling the excitation of fast ion driven TAE (Toroidicity - induced Alfvén Eigenmode) instabilities by varying the injection angle.

The stability of Alfvén Eigenmodes with frequencies up to EAE (above TAE) gaps was simulated numerically with n ranging from 1 to 20. Hybrid MHD/kinetic code NOVA-K was applied. In H-mode and hybrid plasmas the NBI injection angle was varied in order to investigate the possibility of TAE stability control. In both scenarios we found the expected medium to high-n range of TAEs unstable when the NBI was aimed slightly off axis, $10 - 20cm$ vertically away from the midplane. On-axis heating was marginally unstable due to strong central ion Landau damping.

Three ITER AT plasmas were modeled with different values of the shear reversal, which was modified from being close to the hybrid to strongly reversed. We have found that the plasma in the strongly reversed shear configuration is the most unstable. This is due to a much wider TAE gap in the strongly reversed case and generally localized solutions around the q_{min} surface, which is typical close to the maximum gradients of alpha and beam ion pressures.

Overall hybrid and AT plasmas are the most unstable with the growth rates for the unstable modes approaching $3 - 5\%$. H-mode plasmas are the least unstable. Complete stabilization of TAEs seems to be possible in both normal shear and hybrid plasmas by aiming NNBI exactly at the plasma center or far away $50cm$ above/below the axis. In all studied cases NBI ions strongly contribute to instability and are suggested to be used for the TAE stability control in ITER.

*Electronic address: ngorelen@pppl.gov

I. INTRODUCTION

In a thermonuclear deuterium-tritium (D-T) tokamak plasma the $3.5MeV$ alpha particles must be trapped by the magnetic field so that their energy can be transferred, primarily through electron drag, to the background plasma. One purpose of burning plasma (BP) experiments is to demonstrate that this method of self-heating will be the dominant method of heating a plasma that produces fusion energy. However, when the alpha particle partial pressure is significant, a physics issue arises as to whether this pressure is capable of inducing collective behavior that may cause the premature loss of alpha particles. Should this be the case, two major problems may arise: (i) it may become difficult to sustain the plasma parameters close to those required for ignition and (ii) the flux of energetic alpha particles ($\sim 3.5MeV$) to the first wall of the experiment can cause severe wall damage.

Indeed it has been demonstrated in present day (PD) experiments that the collective effects induced from energetic particles can result in premature energetic particle loss. However, it is difficult to extrapolate the results of PD experiments to BP experiments for the following reasons. The fast particle distribution functions are often quite different. In PD experiments the energetic particle distribution are anisotropic, whereas in a BP experiment the distribution function of fusion alpha particles would be isotropic. In addition, in a BP experiment the machine size to orbit width will be significantly larger, and the spectrum (and number) of unstable modes is likely to be broader in a BP compared with PD experiments. Thus even with continued study in PD experiments, extrapolation to reliable predictions for BP experiments may remain uncertain. However, theoretical modeling and simulation can provide predictions of the likely effects of the driven modes.

It is generally believed that the TAEs [3–5] destabilized by fast ions are the plasma waves most likely to cause significant difficulties for the containment of energetic alpha particles in fusion energy generating tokamak experiments. It has been experimentally established that in the presence of a strong enough energetic particle energy density, these modes will induce large losses of fast particles. It is also known that there exists a variety of conditions where these modes are stable or when unstable, do not induce anomalous loss.

This report describes the milestone work to extend the preliminary study [6] to hybrid and AT plasmas. We have performed a systematic study of various plasma scenarios, planned for ITER, in order to determine whether linear instability to the TAEs is expected under specific burning plasma conditions. Specifically, we will study TAE stability for the three proposed scenarios: elmy H-mode, hybrid, and advanced tokamak conditions. TAEs with the toroidal mode numbers up to high 20 will be investigated. With the use of the analytic theory, some extrapolation is possible to other temperature regimes of operation.

The range of toroidal mode numbers of interest is determined by applying simple analytical theory and estimating the mode number dependence of the damping and driving rates [7]. It should be noted that radiation damping becomes a significant damping mechanism when finite Larmor radius (FLR) effects increase for core ions as well as electrons, and becomes a strongly stabilizing effect at $k_\perp \rho_i \sim \sqrt{r/R}$. Here $k_\perp$ is the characteristic radial wave-number of a TAE mode and ρ_i is the bulk ion Larmor radius calculated for ions with thermal velocity $v_T = \sqrt{2T/m}$. This damping mechanism may then compete with the alpha particle drive at moderately high toroidal mode numbers n. The fast particle drive reaches a maximum for n-numbers near

$$nq^2\rho_h/r \simeq 1, \tag{1}$$

where ρ_h is the fast ion Larmor radius, and then beyond this value decreases with increasing n. Depending on detailed parameters, radiation damping may be a significant damping mechanism near the peak of the alpha particle drive.

The stability analysis is done with the hybrid kinetic/MHD code NOVA-K. The input from TRANSP code provides NOVA with the plasma and fast ion profiles. Using the TAE structure calculated by the ideal MHD code, NOVA, the perturbative theory is applied to evaluate the Alfvén eigenmode stability. Several important kinetic damping mechanisms are incorporated into NOVA-K over the years: trapped electron collisional damping [8], ion and electron Landau damping [5], radiative [9] and continuum [10] damping. The fast ion drive is calculated with the orbit and Larmor radius effects included [11].

The application of this stability analysis to ITER shows that one can expect the most unstable mode number to be around $n = 10$ (for both fusion alphas and beam ions) and thus it is important to be able to extend the analysis beyond this number in a systematic way. This is a challenging computational problem as the number of possible eigenmodes increases with n number. At higher n, $n > 10$, the number of grid points has to be increased in both the radial and poloidal directions to resolve the high-m, where $m = nq$, poloidal harmonic structure at the edge. In the simulations grid size ranges up to 400 radial points and 512 poloidal points for $n > 10$.

Note that from Eq.(1) the most unstable toroidal mode number depends on the safety factor value at the point of the strongest pressure gradient, which is typically close to half of the minor radius. This means that the most unstable n numbers in elmy H-mode and in hybrid scenario (see relevant parameters in the next section) are expected to be similar, whereas in the advanced scenario with $q_{min} \sim 2$ the most unstable mode number is expected to be lower. This important property of the TAE stability in ITER is confirmed, numerically in present report.

In Section II we report on the numerical simulations of three nominal ITER plasma scenarios: elmy-H mode [12], hybrid and advanced tokamak plasma (AT, reversed magnetic shear) [13]. The model of the energetic particle distribution function used in NOVA is described in Section III. The stability analysis results for the three ITER scenarios are given in Sections IV, V, and VI. A brief summary and discussion are given in Section VII.

II. DEVELOPING FIDUCIAL NUMERICAL EQUILIBRIA FOR ITER

Even though the elmy H-mode regime was proposed first for the ITER-FEAT project, more recently the hybrid plasma regime has attracted greater attention. It is likely that the hybrid and advanced plasmas will be the main regimes for ITER as they hold the promise of steady-state plasma operations, which is essential for the next step, a demo power plant reactor [13]. The hybrid plasma regime was observed in tokamak experiments [14–16] and has enhanced core confinement compared with the standard H-mode scaling. It offers the potential for ITER to operate at high fusion yield, higher β_n and reduced requirements for the inductive current drive. Several papers have documented encouraging predictions of hybrid plasma performance in ITER based on various predictive models such as the GLF23 [17] and Weiland [18] models.

A. Methods and Modeling Techniques

The TRANSP/TSC combination is used to model ELMY H-mode and advanced plasmas for ITER. The TSC code [1] is used to simulate the start-up and control of the plasma boundary adjusting the shaping and control coils. Several heating and current drive models can be used along with several prediction models (such as GLF23) to derive the evolution of the plasma temperature profiles. The output: time-dependent boundary and plasma profiles are input to TRANSP for more detailed analysis, since TRANSP [2] has more comprehensive and self-consistent methods for computing the equilibrium, heating, and current drive. The TRANSP results for heating and

current drive, if needed, and rotation profiles can be put back into TSC for further iterations to converge on a more accurate model.

TRANSP uses the NUBEAM Monte Carlo package [19] to model alpha heating and neutral beam heating, torque, and current drive. The RF heating and current drive are modeled using SPRUCE [20] and TORIC [21], full-wave, reduced order codes for minority ICRH.

In addition to the standard H-mode case, two classes of advanced plasmas are considered: the hybrid scenario with reduced inductive current and q_{MHD} profile maintained close to, or above unity, and the steady-state AT scenario (see section II B 3) with near zero inductive current. Details of the classes of fiducial ITER plasmas used in this study are summarized in Table I. The H-mode plasma regime is considered to be conservative for achieving $Q_{DT} \equiv P_{DT}/P_{aux} = 10$. The hybrid regime is considered to be a path to similar Q_{DT} but requiring less inductive current, and the Steady State regime aims at longer pulse durations with close to zero inductive current drive. The equilibrium profiles have been submitted to the International Tokamak Physics Activity (ITPA) profile database maintained by the Core Modeling and Database Working Group and the Transport Working Group. The intended uses of the submissions are for code benchmarking and for inputs for down stream analysis. In normal shear H-mode plasma the evolution of the q_{MHD} profile is calculated in TRANSP. To model effects of sawteeth, sawteeth crash times are assumed, and the TRANSP sawtooth model is used to helically mix the plasma current and fast ion profiles at the crash time if $q_{MHD}(0) < 1.0$. Otherwise, poloidal field diffusion is calculated assuming neo-classical resistivity and bootstrap current, and driven currents in the case of NBI. The sawteeth simulations resulting from this analysis generally agree well with experimental observations in plasmas, such as L-mode, H-mode, and supershots with monotonic or mildly reversed q_{MHD} profiles. The profile for ITER-FEAT would be affected by 1 MeV NNBI. If the sawtooth model is not invoked, the central values for q_{MHD} are predicted to evolve in time to ≈ 0.7.

	I_p	I_{boot}	I_{nnbi}	I_{Oh}/I_p	$n_e(0)$	f_{GW}	T_e	P_{dt}	$\beta_\alpha(0)$
units	(MA)	(MA)	(MA)		$(10^{20}/m^3)$		(keV)	(MW)	(%)
ELMy	15	2.7	1.1	0.70	1.1	0.80	22	403	0.6
hybrid	12	2.8	4.5	0.32	0.6	0.47	33	305	1.3
AT	9	4.3	4.3	0.0	0.6	0.63	33	305	1.3

Table I: *Typical plasma parameters for three nominal ITER scenario*

One of the uncertainties of the viability of hybrid plasmas in ITER is whether suitable q profiles can be created and maintained. The q profiles in present hybrid plasmas have minimum values close to, but often above, unity. Either no or small sawteeth are observed. Often benign Neoclassical Tearing Mode (NTM) activity is observed. There is a speculation that NTM or dynamo effects create special q profiles required for hybrid plasmas. This raises concern that the required q profiles might not be accessible in ITER unless special current drive such as Electron Cyclotron (ECCD) or Lower Hybrid (LHCD) is used to control q. An alternative is to use off-axis beam-driven current (NBCD).

It was pointed out recently [22] that NBCD resulting from below-midplane NNBI aiming can maintain q above unity. The ability to alter the aiming in ITER from shot to shot is being planned. The TSC and TRANSP codes are used for time-dependent integrated predictive modeling of ITER plasmas within the region extending from the core out to the top of the edge pedestal. The modeled plasmas have reduced plasma current and high β_n relative to the baseline H-mode plasmas [12] (I_p=12 vs 15 MA and β_n near 3 vs 1.8). The reduced I_p and increased β_n imply reduced Ohmic current and the increased bootstrap current. These allow the NBCD to have a significant effect on the central q-profile. Below-axis aiming into hybrid plasmas is predicted to sustain q above unity

for long ($> 800s$) durations. The indication that NBCD can maintain q above unity might obviate the need for alternatives such as ECCD or LHCD and benign NTMs to affect the q profile.

We also studied the effects of variation of the NNBI aiming into standard H-mode plasmas in ITER (with $I_p = 15MA$ and $\beta_{norm} = 1.8$, see section **??**) and found that there is little effect on the central q (as shown) unless the sawtooth period is long (much greater than $10s$).

The auxiliary heating power for the H-mode and hybrid plasmas are assumed to be 16.5 or $33MW$ of D-NNBI (with one or two beam lines), and up to $20MW$ of ICRH at $53MHz$ (tuned to the He^3 minority resonance near the plasma center). The ITER design for the NNBI sources allows for a rotation in the vertical plane allowing the footprint of the beam in the plasma to vary by approximately $50cm$ vertically from shot to shot. Injection of NNBI is shown in Figure 1.

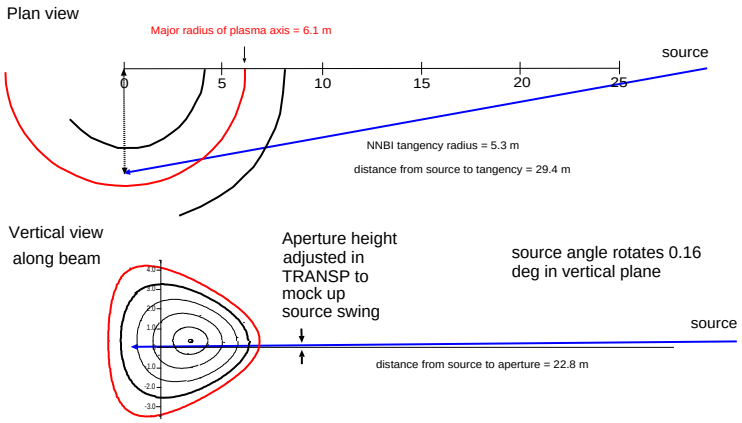

Figure 1: *Schematic of NNBI in ITER. a) top view, b) side view*

The following subsection present the main plasma profiles relevant to the AE stability study we performed, including the effect of off-axis NBCD and variations of the safety factor profile.

B. Plasma profiles for three scenarios

1. Standard, elmy H-mode plasmas

The following table gives a list of TRANSP run numbers and a number of their representative profiles shown in the figures hereafter. In this set of plasmas the injection angle was varied so that the NBI is aiming on plasma center if $Y = 0$ and off (below) center.

TRANSP id	# in figure legend	Y(cm)
20000T03	1	-50
20100T02	2	-38
20000T02	3	-10
20100T03	4	-20
20000T01	5	0

Table II: *A list of TRANSP runs along with the number of the profile shown in the next figures. Y is the vertical displacement of the beam line at its nearest point to its tangential radius.*

In elmy H-mode plasma there is little effect on the central q from the variation of the injection angle unless the sawtooth period is long (much greater than $10s$) as can be seen from figure 2 (right).

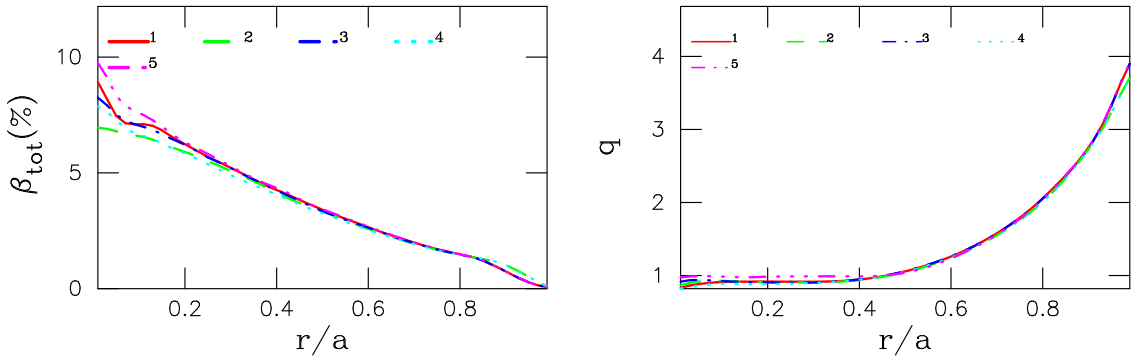

Figure 2: *Total plasma beta (left) and safety factor profile (right) for elmy H-mode ITER plasmas*

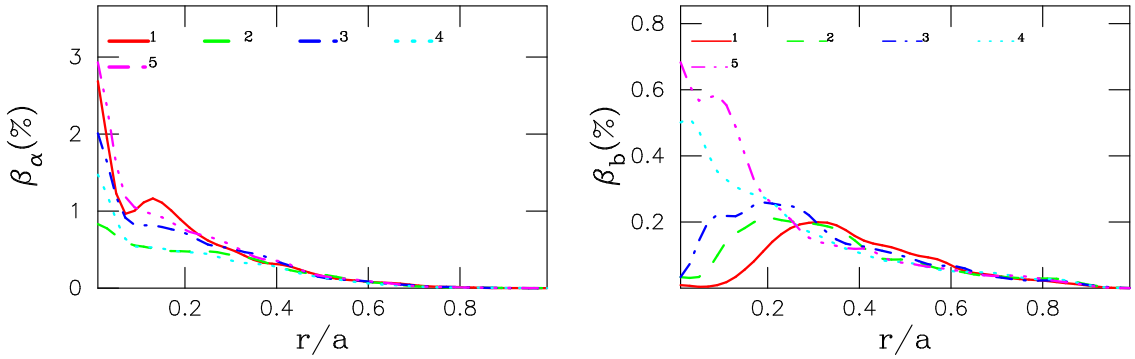

Figure 3: *Fusion alphas and NNBI confined ion betas*

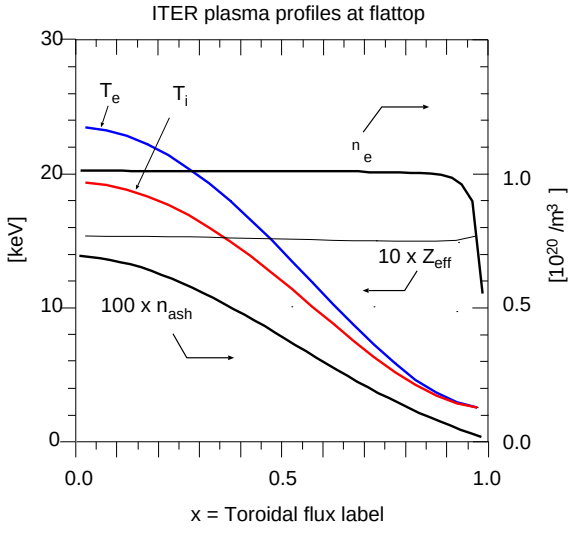

Figure 4: *Profiles of the ITER H-mode plasma paremeters. The He^4 ash density times 100 is computed from the fast alpha thermalization assuming R_{ash} = 20% and D_{ash} = 0.8 [m^2/s], and is in steady state at the time shown.*

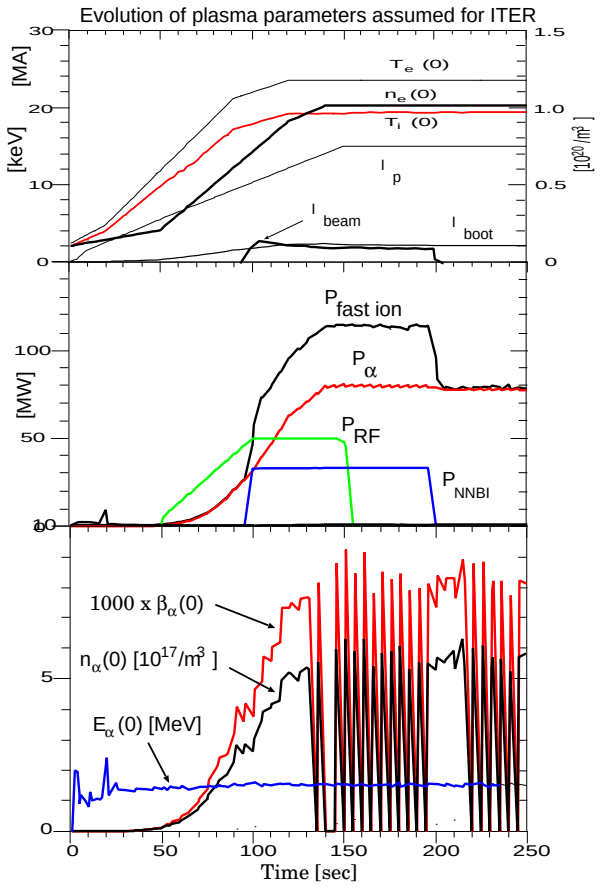

Figure 5: *Time evolution of parameters in the normal shear elmy H-mode ITER plasma. The alpha parameters in c) are volume-averaged out to the* $x = 0.1$ *flux surface to reduce Monte Carlo fluctuations.*

The distribution function is simulated in TRANSP using the Monte-Carlo model for each equilibrium (see example in figure 6 for elmy plasma) and is fitted to a special parametric dependence, section III, in NOVA-K code [6]. Its velocity space dependence is not very sensitive to the injection geometry.

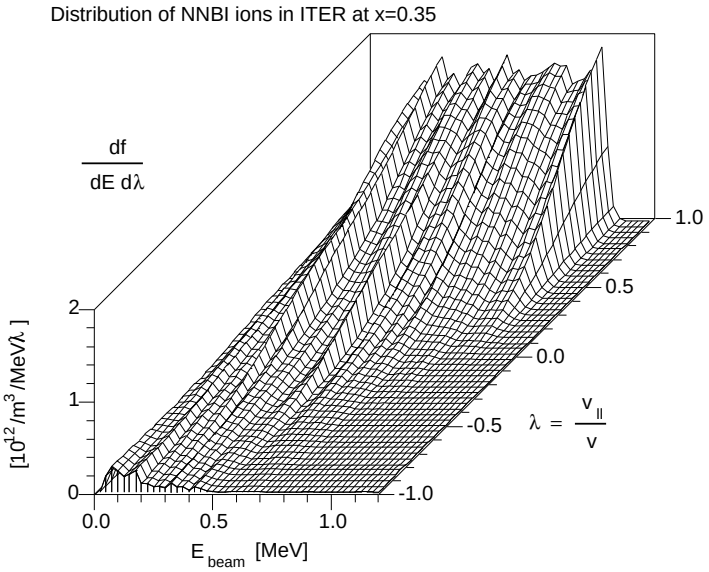

Figure 6: *Distribution of the ITER NNBI beam ions in energy and pitch angle at* $x = 0.35$*, averaged over poloidal angle, computed by the TRANSP Monte Carlo model. The neutrals are injected at 1MeV with* $v_{\|}/v \simeq 1$*, and the beam ions become more isotropic as they slow down.*

2. Hybrid scenario plasma

Following is the table of TRANSP identification run numbers and a number of their representative profiles shown in the figures hereafter for the hybrid plasmas.

TRANSP id	# in figure legend	Y(cm)
40500T04	1	20
40500T03	2	10
40500A06	3	-20
40500T02	4	-40
40500A04	5	3

Table III: *A list of TRANSP runs along with the value of NNBI vertical displacement, Y, of its injection line at its nearest point to its tangential radius*

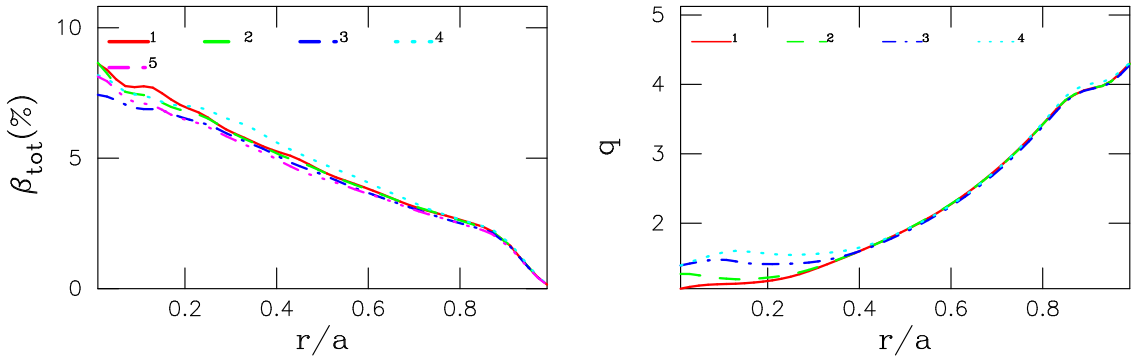

Figure 7: *Total plasma beta (left) and safety factor profile (right) for hybrid scenario ITER plasmas*

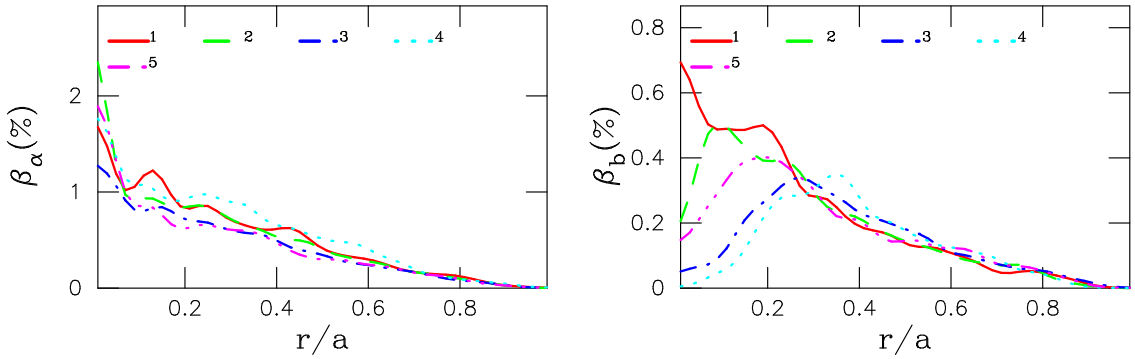

Figure 8: *Fusion alphas (left) and NNBI confined ion betas (right) for hybrid scenario ITER plasmas*

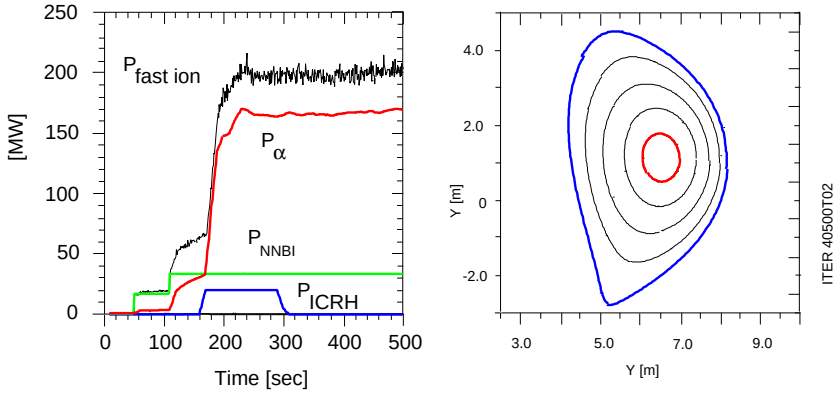

Figure 9: *Heating powers from fusion alpha particles, NNBI, and ICRH (left). Poloidal section showing surfaces of constant toroidal flux (right)*

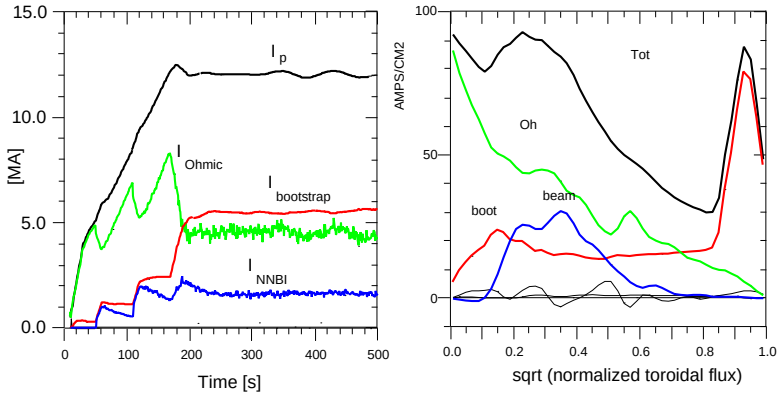

Figure 10: *Plasma currents (left) and profiles (right) in an ITER hybrid plasma*

3. Advanced tokamak (reversed shear) plasma scenario

As the effect of the variation of the NNBI inclination angle on TAE stability will be covered in elmy H-mode and hybrid plasmas, it seemed interesting to perform a separate study to investigate how different q-profiles affect the AE stability. Variations in q-profiles are achieved in AT ITER plasmas via timing of application of ICRH, changing energy of NNBI and Ohmic current. These runs are based on TSC runs with ad hoc transport since no adequate GLF23 temperature simulation has been found. In addition, slightly peaked electron density profiles are assumed. Also, we explored the possibility of having high beta normal according to the table.

TRANSP id	# in figure legend	$Y\,(cm)$	β_N	$I_p\,(MA)$	$E_b\,(MeV)$	$n_e/n_{Greenfield}$	Fusion Power (MW)
60000T02	1	-40	3.3	8-9.5	1	0.82	493
60000T04	2	-20	3.3	8-9.5	0.8	0.97	400
40000B11	3	-20	2.3	12	1	0.47	315

Table IV: *A list of TRANSP runs along with the value of NNBI vertical displacement, Y, and other relevant parameters for AT plasmas*

Radial plasma profiles are given in Figures 11 and 12. One can see that stronger reversed shear is achieved by having off-axis beam ion pressure profiles (and current drive) as in the case of TRANSP run $40000B11$ (plasma #3).

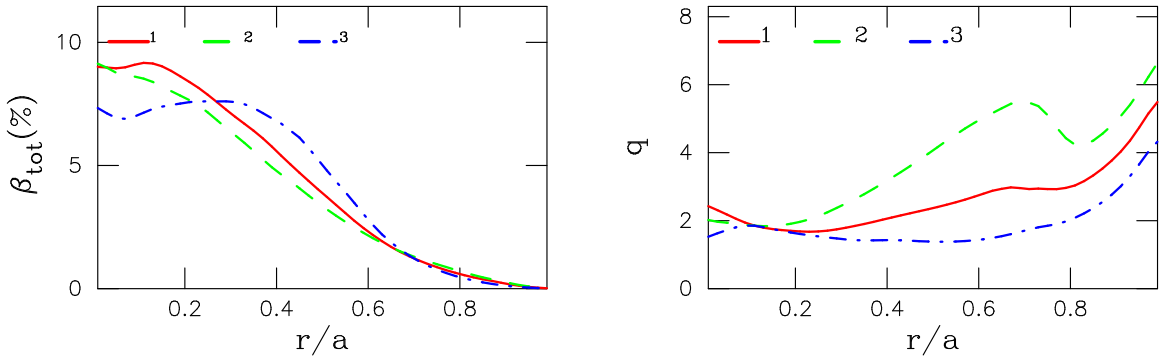

Figure 11: *Total plasma beta (left) and safety factor profile (right) for reversed shear ITER plasmas*

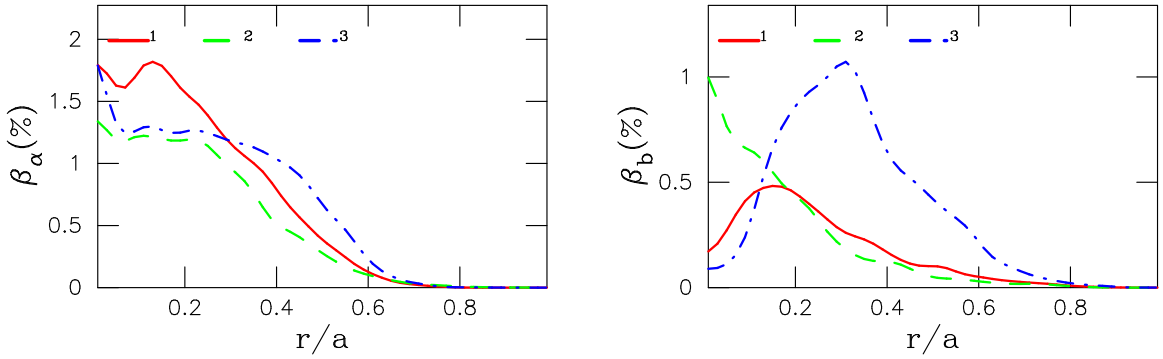

Figure 12: *Fusion alphas, β_α, and NNBI confined ion, β_b, betas*

III. NBI ION DISTRIBUTION FUNCTION MODEL

Previous studies [6, 7] have shown that neutral beam ions contribute as strongly as fusion alpha particles to the TAE growth rate. Hence, the model for the beam ion distribution function is of critical importance. We outline and emphasize the distribution function model in this section, specifically we compare it with the results of the improved TRANSP statistics Monte-Carlo package.

If the injected distribution function is narrow in pitch angles, which is the case with NBI ions in ITER, the model to describe the distribution function of beam ions, f_b, and used in NOVA calculations [6] can be applied. It was proposed that f_b can be expanded in terms of the Legendre polynomials $P_l(\chi)$, which are the eigenfunctions of the Lorentz collisional scattering operator in the kinetic equation for f_b: $f_b = \sum_l a_l(\tau) P_l(\chi)$, $\tau = -(1/3)\ln\left[\left(1+v_*^3/v_{b0}^3\right)/\left(1+v_*^3/v^3\right)\right]$, v_{b0} is the injection velocity (at $\tau = 0$), $\chi = \mathbf{B}\cdot\mathbf{v}/vB$, v_* is the critical velocity at which the ion collisional drag becomes comparable with the drag on electrons. The solution at a given variable τ can be easily obtained

$$\phi(\chi) = \sum_l a_{l0} e^{-l(l+1)\tau} P_l(\chi), \tag{2}$$

where $a_{l0} = (l+1/2)\int_{-1}^{+1} P_l S(\chi-\chi_0)\, d\chi$. Practically $l \geq 26$ are required for good accuracy for the source term in the form $S = e^{-(\chi-\chi_0)^2/\delta\chi^2}/\delta\chi\sqrt{\pi}$, at $\chi_0 = 0.7$ and $\delta\chi = 0.12$. Pitch angle

distribution, accounting for the trapping region, is obtained by substituting solution of Eq.(2) into the form

$$f_\chi = \begin{cases} \phi(\chi) - \frac{1}{2}\phi(2\chi_{s+} - \chi), & \text{counter-going ions, } \chi < -\chi_s \\ \frac{1}{2}\phi(-\chi) + \frac{1}{2}\phi(\chi), & \text{trapped ions } -\chi_s < \chi < \chi_s \\ \frac{1}{2}\phi(2\chi_{s+} + \chi), & \text{co-going ions } \chi_s < \chi \end{cases} . \tag{3}$$

This accounts for proper boundary conditions at the trapped-passing region separatrix and utilizes the image method for the image beam ion sources in order to include particle reflection from pitch angle boundaries [6]. Since this technique is not exact the resulting distribution may have discontinuities if its pitch angle width is large (or $\tau \geq 1/2$). We proposed a method which results in a good approximation to the exact solution. First, we account for the discontinuity by making the distribution continuous and renormalize it to conserve particles, which we denote f'_χ. Second, we force it to become isotropic, $f_\chi = 1/2$, at $\tau \to \infty$. Applying this procedure, the pitch angle part of the distribution function is given by

$$f_\chi = \frac{4\tau^3 + f'_\chi}{8\tau^3 + 1}, \tag{4}$$

where parameters are adjusted for better agreement with the exact solution, which we find by performing Monte-Carlo simulations. We should note, however, that adjustable parameters do not depend on the plasma parameters. The comparison with numerical simulations is shown in Fig. 13. It is notable that in both cases with low and high statistics, model distribution reproduces functional pitch angle dependencies of the numerical TRANSP simulated distribution. The advantage of using the model distribution is that it allows taking appropriate derivatives, which are apparently smooth.

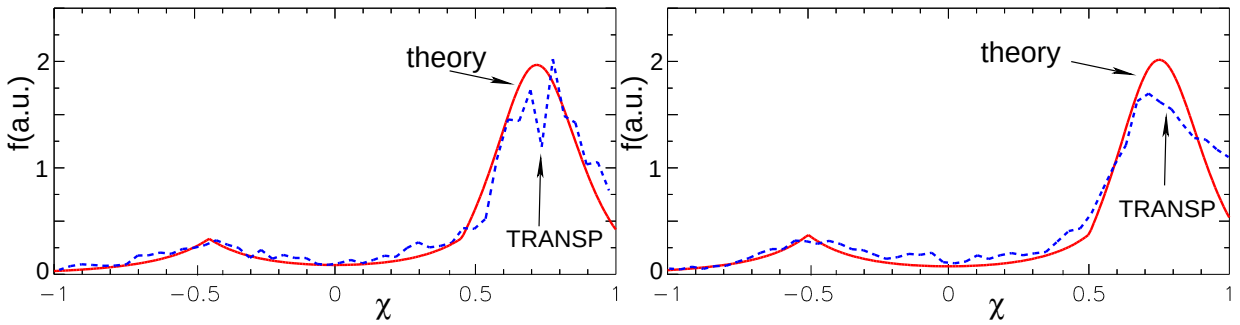

Figure 13: *Results of applying the model of the beam ion pitch angle distribution function as given by Eq.(3) (theory curve) and its comparison with the TRANSP simulations (TRANSP curve) for low statistics run, $N = 10^3$ particles (left figure, distribution function is averaged over $r/a = 0.3 - 0.7$ range in minor radius) and high statistics run, $N = 10^5$ particles. In this case we used the low aspect ratio approximation for parameters $\delta\chi = 0.12$ and $r/R = 1/6$.*

It is know that in the drift, guiding center approximation equilibrium particle distribution function is a function of particle integrals of motion: velocity v, adiabatic moment $\mu = v^2\left(1 - \chi^2\right)/2B$, and toroidal momentum $P_\varphi = v_\varphi R/\psi_1 - e_i\psi/\psi_1 2\pi$, where ψ_1 is the poloidal magnetic flux at the last closed magnetic surface. This set of variables is adopted in NOVA-K [11]. It is compatible with the above description of the distribution function, provided the pitch angle $\chi = \chi\left(v, P_\varphi, \mu\right)$ is taken at the largest major radii (for definitiveness) over the particle drift orbit, that is when particle crosses the midplane. The following figures show examples of the distribution function of

alphas and beam ions taken at half of their birth (injected) energy as they are approximated by the model described in this subsection. One can see that the distribution of alphas is more isotropic then the distribution of beam ions injected into the narrow pitch angle range.

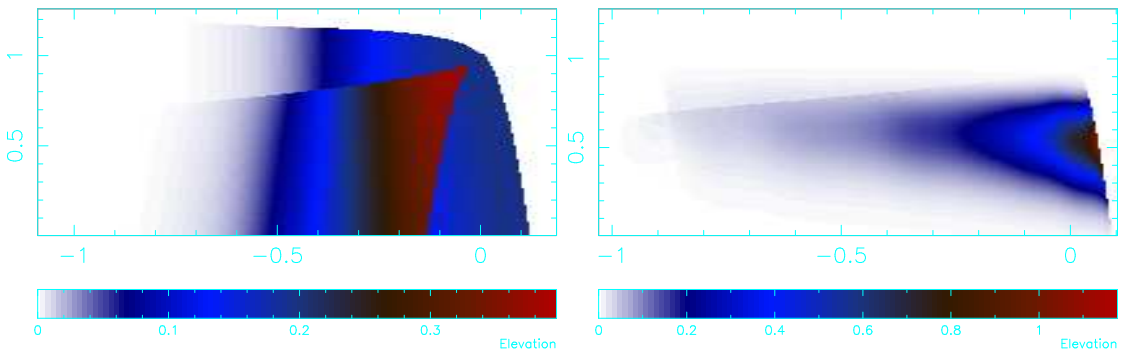

Figure 14: *Fusion alphas (left figure) and NNBI confined ions (right figure) equilibrium distribution functions plotted as contour maps in P_φ (horizontal axis) and $\lambda = 2B_0\mu/v^2$. (For details of the phase space representation see Ref.[23].) Plotted pitch angle distribution function is normalized in such a way that its integral over the velocity phase space is 1. The particle position in the phase space can be explained taking left figure as an example (alphas). The upper parabola is the region of trapped alphas. The parabola "looking" downward from the (0,1) point encompasses the region of cogoing passing alphas. The region on the left from this parabola overlap both co and counter going passing alphas.*

IV. LOW- TO HIGH-N TAE STABILITY IN NORMAL SHEAR ITER PLASMAS

A. Ideal MHD continuum

As an example we compute and present MHD continuum for ITER plasmas with slightly off-axis NBI heating, which is the most unstable studied H-mode case #20000T02 (figure 15). Another example is for the less unstable plasma with stronger off axis beam injection #20100T03 (figure 16) with NBI aiming $20cm$ below the magnetic axis. These plasmas have sawteeth, which are reflected in the low shear region inside the $r/a = 0.5$ surface. The plasma current was ramped up relatively fast in these plasma configurations, Fig.(5). This resulted in a low shear central region, whereas in previous studies [6] the low-shear region was located near $r/a = 0.5$ giving rise to TAEs localized in that region, and determining the stability properties. As one can see from Figs. 15 and 16, localized TAE modes are present in the low shear region. Other global modes, which couple low shear and the plasma edge regions, were also found but are subject to stronger damping mechanisms, such as continuum and radiative damping, which are large at high safety-factor shear, typical for the plasma edge.

B. AE stability

The list of analyzed plasmas in this case is given in Table II. We present stability simulation results with α-particles only and with alphas and beams contributing to the drive in Figs. 17, 18, and 19. Negative (positive) growth rates indicate that the modes are stable (unstable).

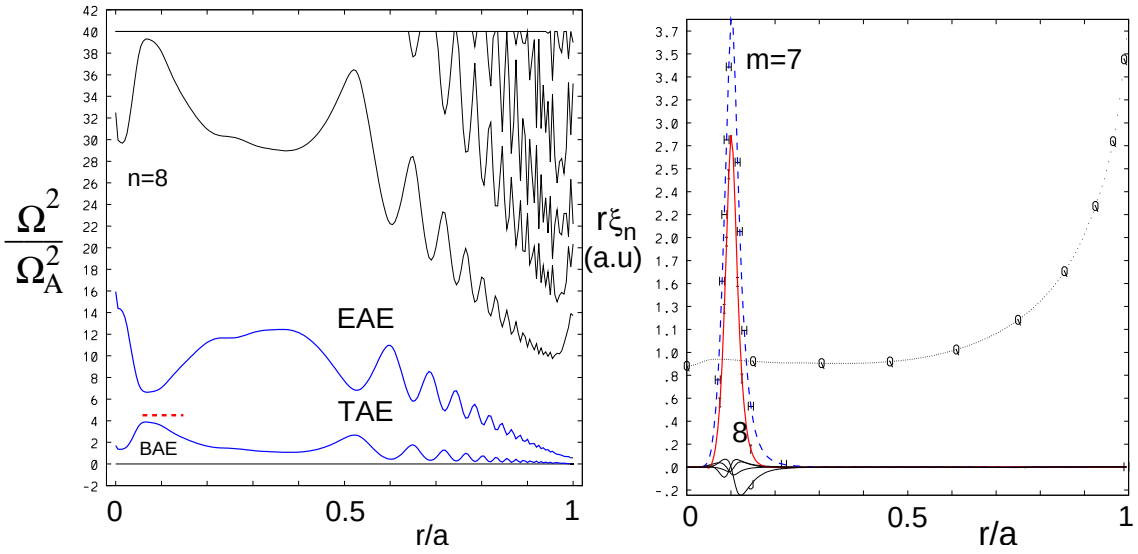

Figure 15: *Ideal MHD continuum for ITER normal shear H-mode plasma run* #20000T02 *(left figure) and the most unstable core localized TAE poloidal harmonic radial structure for this case with NBI aiming* 10cm *below the magnetic axis. The radial extent of this mode is shown in the left figure as a dashed line corresponding to the normalized TAE eigenfrequency.*

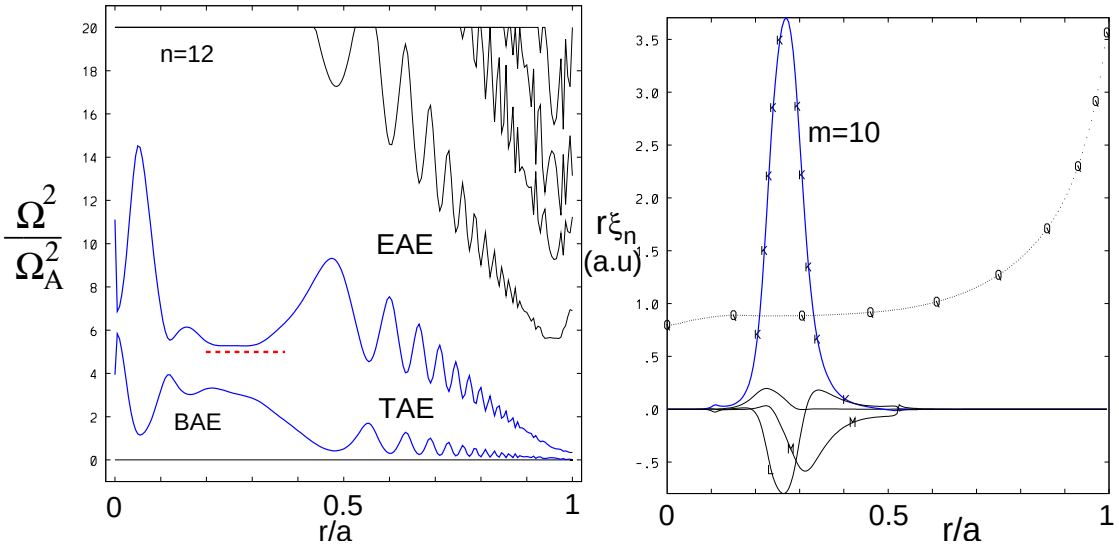

Figure 16: *Ideal MHD continuum for ITER normal shear H-mode plasma run* #20100T03 *(left figure) and the marginally stable but radially wide low shear localized TAE poloidal harmonic radial structure for this case with NBI aiming* 20cm *below the magnetic axis. The radial extent of this mode is shown in the left figure as a dashed line corresponding to the normalized TAE eigenfrequency.*

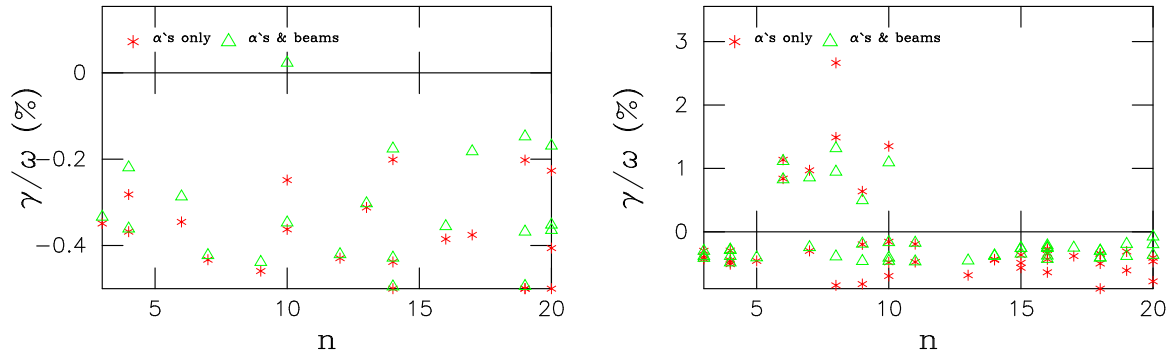

Figure 17: *Toroidal mode number dependence of the AEs growth rates for the instabilities driven by alpha particles only (∗ points), and driven by both NBI ions and alpha particles (△ points). Results are for on-axis* $Y = 0$ *NBI, ITER TRANSP run #*$20000T01$ *(left figure) and for the run #*$20000T02$ *with* $Y = -10cm$ *(right figure).*

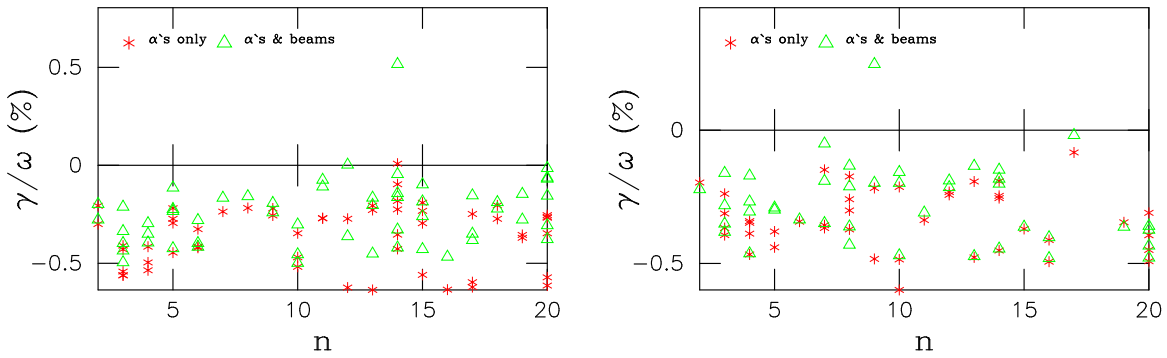

Figure 18: *The same as in figure 17 but for* $Y = -20$*, #*$20100T03$ *run (left figure) and for the run #*$20100T02$ *with* $Y = -38cm$ *(right figure).*

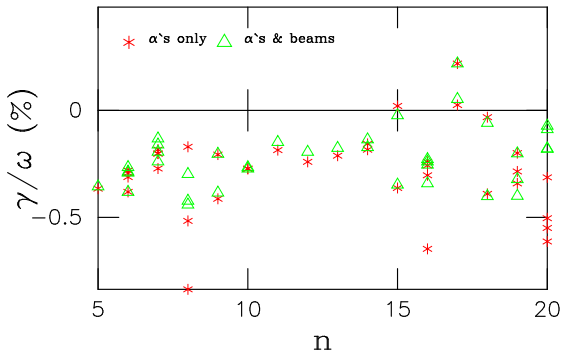

Figure 19: *The same as in figure 17 but for* $Y = -50$*, #*$20000T03$ *run*

Summarizing the TAE stability for the normal shear H-mode plasma we plot total TAE growth rates vs. vertical deviation of the NBI aiming point from the magnetic axis, Fig. 20. On-axis

beam injection seems to be stable due to higher ion Landau damping, whereas aiming $10cm$ below the axis represents the most unstable case with the growth rates reaching 2.5% due to centrally peaked α-particle pressure profile. This is a result of the geometrical effect of the NBI. Aiming below the midplane at lower values of Y shows stabilizing effects too, as the beam is injected into regions with higher shear and stronger radiative and continuum dampings. The unstable TAEs are localized to the region of low shear within $r/a < 0.5$ in all cases of H-mode plasmas.

It seems likely that such localized TAEs will not result in any significant effects on fast ion confinement, but may transport them radially toward the edge where such phenomena as TAE avalanches could be formed.

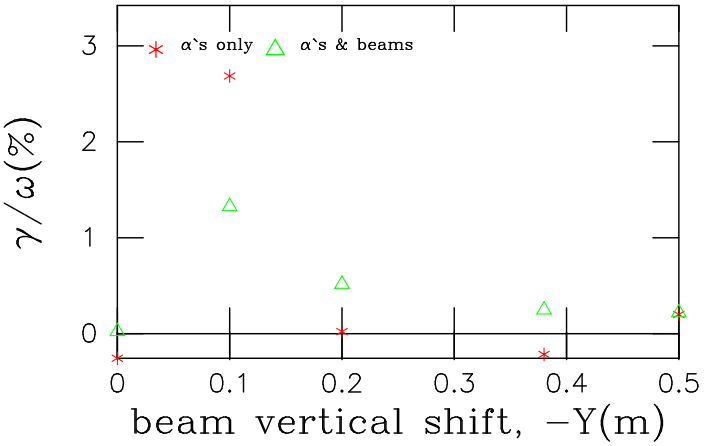

Figure 20: *Most unstable TAE growth rates vs. vertical deviation of the beam injection from the magnetic axis*

V. TAE STABILITY IN HYBRID SHEAR DISCHARGES

Five plasmas of the list reported in section II, Table III, are analyzed in this section. This time we set up the injection geometry in such a way that the beam is aiming above and below the magnetic axis, which is different to the normal shear plasma, where injection was below or into the midplane.

Hybrid plasma differs from the monotonic q-profile, elmy H-mode plasma in a way that the q-profile has more complex structure. As one can see from Fig. 7 (right) of section II, the current drive (mostly from NBI) introduces local reversed shear near the plasma center. This is important equilibrium property for the stability study as the region of low shear determines a potential location and radial extent of such modes as TAEs and RSAEs.

A. Ideal MHD continuum and TAE structure

In Fig. 21 we show the MHD continuum for ITER plasma with off-axis NBI aiming at $10cm$ above the midplane, which is used to study the sensitivity of the TAE stability to the inclination angle. Two most unstable modes in this case are also shown in that figure. Both are close to the

low shear region and are unstable. Such a case, when several modes closely located can potentially lead to resonance overlap and strong radial transport of fast ions.

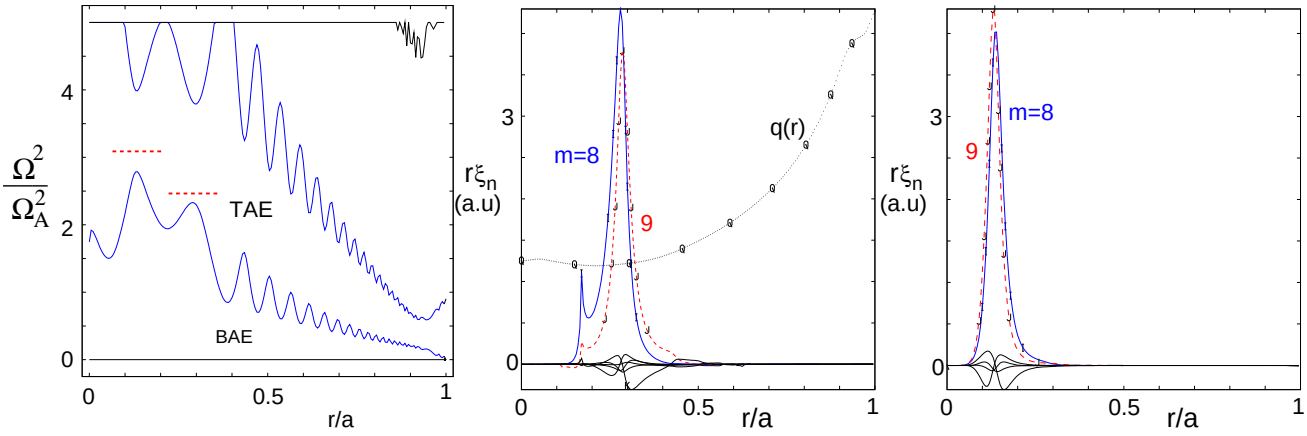

Figure 21: *Ideal MHD $n = 7$ continuum for ITER hybrid plasma run #40500t03 (left figure) and two most unstable low shear localized TAE poloidal harmonic radial structures for the case with NBI aiming 10cm above the magnetic axis. Center figure represents the radial structure of TAE with $\Omega^2/\Omega_A^2 = 2.41$ and right figure corresponds to TAE with $\Omega^2/\Omega_A^2 = 3.09$, where NOVA uses normalization $\Omega_A = v_{A0}/q_a R$. The radial extent of these modes is shown in the left figure as dashed lines. Vertical position of these lines corresponds to the normalized eigenfrequency.*

One problem we had to address when we modeled the hybrid plasma is the non-monotonic radial dependence of beam ion and fusion alpha beta profiles. The profiles are given in Fig. 8. The fluctuations in the radial profiles of fast ions result from the Monte-Carlo noise of the TRANSP code. In order to cope with this we developled a smoothing procedure. Fitted profiles for fast ions used in NOVA simulations are shown in Fig. 22. This way we avoided overestimation of localized TAE growth rates, when their amplitude was peaked at the local strong fast ion pressure gradient region.

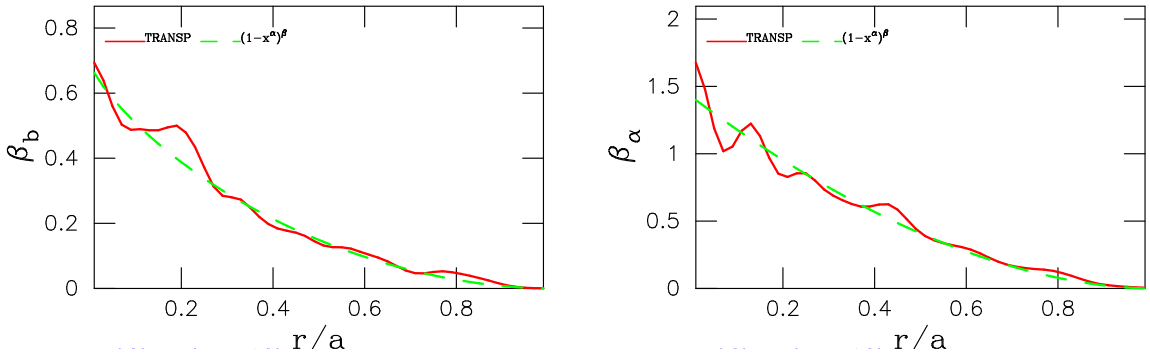

Figure 22: *Example of the TRANSP produced NBI (left) and fusion alphas (right) beta profiles (in %) for ITER hybrid plasma run 40500T04. Shown as solid lines are the profiles from TRANSP code. Shown as dashed lines are the fitted profiles, used in NOVA simulations.*

The beam ion distribution function model is described in section III, Eqs.(2,3,4). It turns out that the key parameters for the distribution function are not sensitive to the plasma scenario because of the large size of the plasma and relatively weak change in the inclination angle of NBI. The same parameters for the beam ion distribution function are used in this section simulations.

B. TAE stability in hybrid plasmas

We present stability simulation results with α-particles only, and with alphas and beams contributing to the drive in Figs. 23, 24, and 25 for five hybrid plasmas. Negative (positive) growth rates indicate that the modes are stable (unstable). In general hybrid plasmas are more unstable than H-mode due to higher fusion alpha pressure. This is in turn due to a larger plasma temperature, which is about $T_{i0} = 29keV$, whereas it is $T_{i0} \simeq 20keV$ in H-mode plasmas. So fusion alpha particle beta increases stronger with T_i than the damping rate from thermal ions (Landau damping).

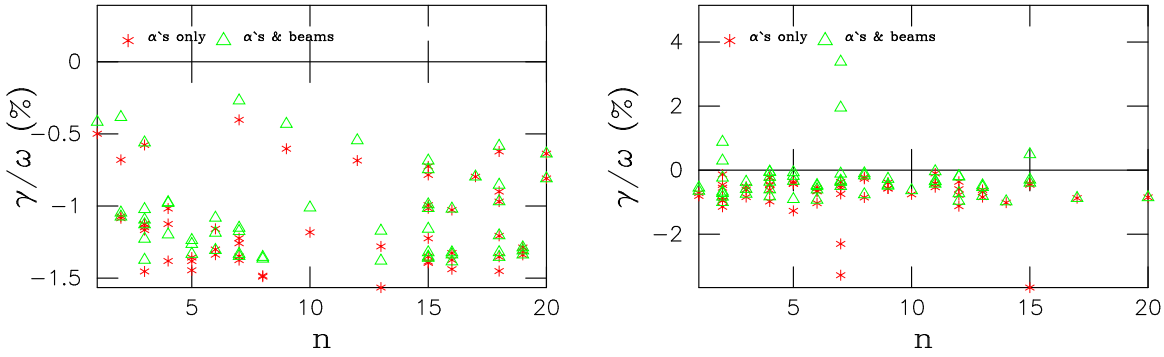

Figure 23: *Toroidal mode number dependence of the AEs growth rates for the instabilities driven by alpha particles only ($*$ points), and driven by both NBI ions and alpha particles ($\triangle$ points). Results are for NBI aiming $Y = 20cm$ above plasma axis, ITER TRANSP run #40500T04 (left figure) and for the run #40500T03 with $Y = 10cm$ (right figure).*

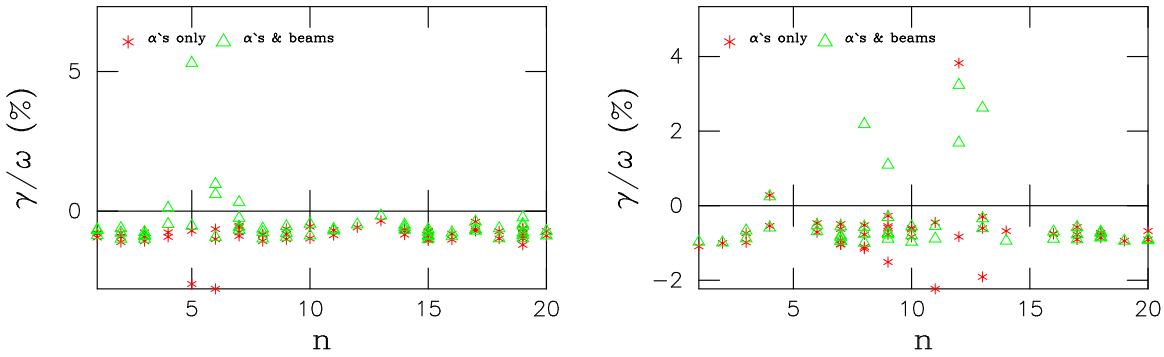

Figure 24: *The same as in figure 23 but for $Y = -20cm$, #40500A06 run (left figure) and for the run #40500T02 with $Y = -40cm$ (right figure)*

For the hybrid plasmas we plot the maximum growth rate of TAEs vs. vertical deviation of the NBI aiming point from the magnetic axis, Fig. 26. Consistent with previous studies, the on-axis beam injection seems to be most stable. Aiming $10cm$ above produces instability and aiming $20cm$ above the axis produces TAE stable plasma. Aiming $20cm$ and $40cm$ below the axis again makes the plasma unstable. The unstable TAEs are localized to the region of low shear within $r/a < 0.5$ in most of the cases of hybrid plasmas investigated. However, weakly unstable global

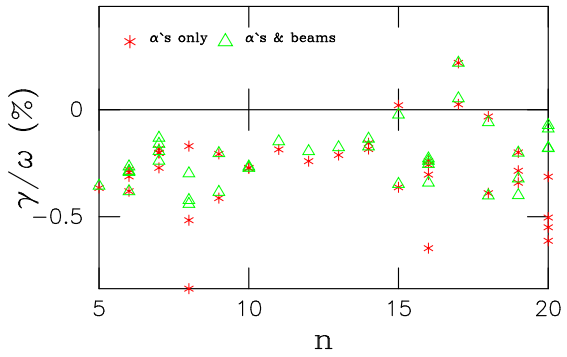

Figure 25: *The same as in figure 23 but for $Y = 3cm$ (on-axis heating), #40500A04 run*

TAEs outside $r/a = 0.5$ are also present. This means that in hybrid plasmas fast ion transport can be more significant as the center of the plasma and the plasma edge are coupled via global TAEs. More studies have to be done for the nonlinear TAE problem and associated global radial transport of fast ions. NOVA is an important tool in such a way that it can predict which n's are most unstable.

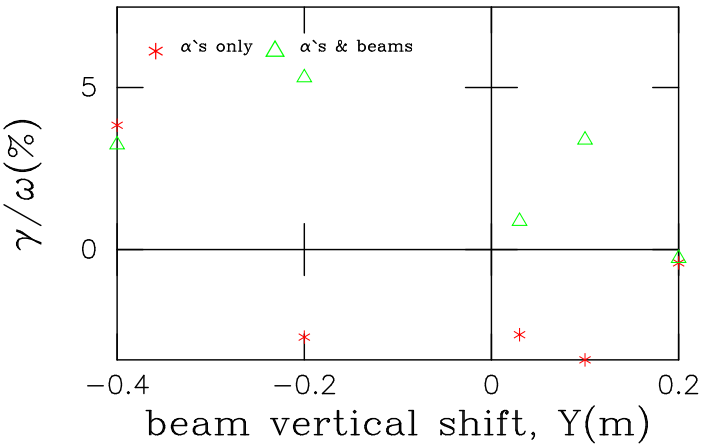

Figure 26: *Most unstable TAE growth rates vs. vertical deviation of the beam injection from the magnetic axis for hybrid plasma*

VI. TAE STABILITY IN THE REVERSED SHEAR DISCHARGES

In this section we scan the safety factor profiles from weakly reversed, close to the hybrid scenario (studied in previous section) to a strongly reversed, steady state. NNBI aiming was approximately the same and was chosen to optimize the beam current drive. The main variation in the TAE stability is coming from the q-profile variations. In particular the location and the wide radial extent of the low shear region result in the more unstable TAEs. That is why this particular study of the TAE stability is important for the planning of AT plasma experiments in ITER.

A. Ideal MHD continuum and TAE spectra

In Figure 27 we show the MHD continuum for ITER AT plasmas of interest. We note two distinct features of these continua.

First, plasmas 1 and 2 have much wider BAE gap. This produces an upshift to the TAE frequency range continuum, so that the TAE gap becomes less aligned radially. This is expected to have a stabilizing effect by introducing more continuum damping. In addition, higher beta of plasmas 1 and 2 downshifts TAE eigenfrequencies into the continuum especially near the center. This stabilizing effect means that certain TAEs will not exist in those plasmas.

Second, comparing Figures 27 with q-profiles of Figure 11 (right) we can also conclude that the widest TAE gap corresponds to the safety profile with the widest region of the low shear, plasma #3, Figure 27 (3). This implies that such plasma can be prone to stronger TAE instabilities. We confirmed this by rigorous numerical study.

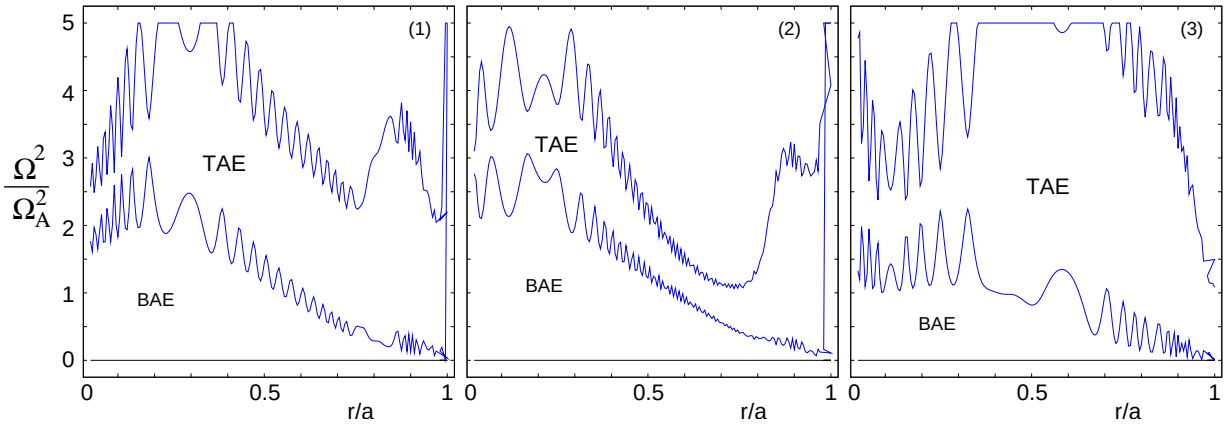

Figure 27: *Ideal MHD* $n = 10$ *continuum for ITER reversed shear plasmas numbered* $\#1, 2, 3$ *in table IV. Frequencies are normalized to* $\Omega_A = v_{A0}/q_a R$.

Figures 28 summarizes our study. As we expected the least unstable case is plasma #2 (60000T04, stability shown in Fig. 28, center), which has the most narrow TAE gap, Fig. 27, center. Thus, stronger continuum damping is expected. In the opposite case of the strong reversed shear plasma, #3, (40000B11, stability shown in Fig. 28, right) TAE modes are localized in the strongest alpha particle and beam ion pressure gradient as can be seen in Fig. 12.

Most interesting is that strongly RS plasma, in addition to having a few unstable localized solutions, such as $n = 11, 12$, we found many weakly unstable, but global modes, both TAEs and EAEs (ellipticity induced Alfvén eigenmodes). An example of the most unstable $n = 11$ TAE and weakly unstable $n = 2$ EAE are shown in Fig. 29. Due to their global mode structure, such multiple instabilities appearing at $n = 1$ to $n = 11$ can be very dangerous for fast ion confinement due to the expected closeness of their wave-particle resonances to each other in the phase space. As a result, even with small mode amplitudes (small drive), resonances can overlap and enhanced transport may develop, possibly causing such effects as radial transport avalanches.

We present the example of the stability calculations for the modes shown in Fig. 29 in Table V. In this cases beam drive seems to dominate the instability. This is due to strong peakedness of its pressure profile outside of the plasma center.

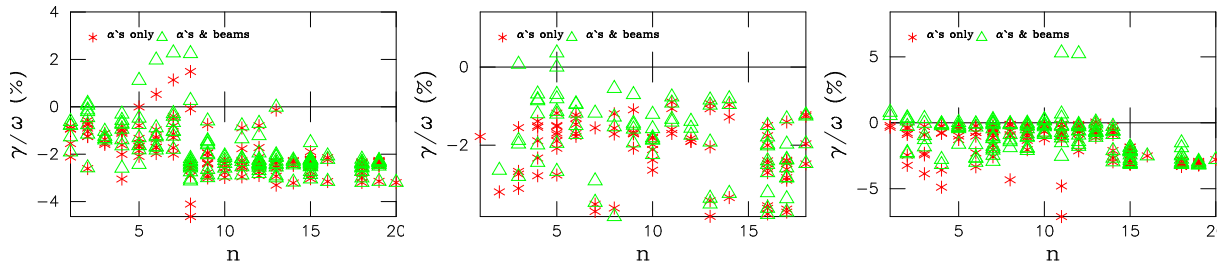

Figure 28: *Toroidal mode number dependence of the AEs growth rates for the instabilities driven by alpha particles only (∗ points), and driven by both NBI ions and alpha particles (△ points). Results are for ITER reversed shear plasmas numbered #1, 2, 3 listed in Table IV, shown in left, center and right figures, respectively.*

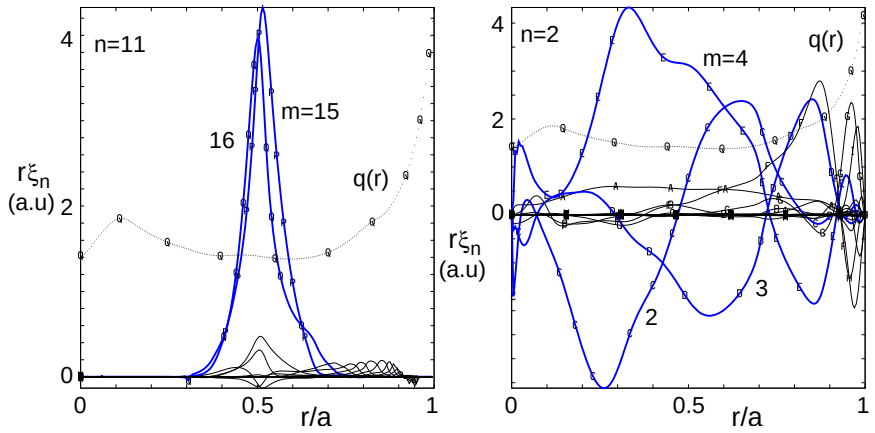

Figure 29: *Left figure represents the radial structure of the most unstable localized TAE in strongly reversed ITER AT plasma #3. Left figure TAE has* $n = 11$ *and* $\Omega^2/\Omega_A^2 = 2.12$*. Right figure corresponds to EAE with* $\Omega^2/\Omega_A^2 = 6.7$ *and* $n = 2$*, which is weakly unstable, but more global.*

B. 2D visualization of wave particle resonances

The effect of the anisotropic distribution function on the stability of AEs can be understood with the help of the visualization of the phase space positions of the wave particle resonances. They are determined by the mode location and the characteristic frequencies of particle drift motion. We show one example of such resonances plotted in Fig. 30 in the same plane as in Figs. 14. The most of the drive is coming from the same phase space region of alphas and beam ions, which is $P_\varphi = -0.1$ and $\lambda \simeq 0.5$. This is due to a very similar characteristics of alpha and beam ion drift motion, such as alphas birth and beam injection velocity, and transit frequencies. However, it is interesting to observe that alpha particles have much wider interaction with the mode in comparison with beam ions which have more narrow distribution function. This has implications that beam ions can drive the TAE at the phase space position of their injection whereas alphas interacting with the same mode can be redistributed radially in other phase space regions, such as $P_\varphi = -0.3$, $\lambda \simeq 1$ in our example.

n	Ω^2/Ω_A^2	$f(kHz)$	$\gamma_{iL}/\omega\,(\%)$	$\gamma_e/\omega\,(\%)$	$\gamma_{continuum}/\omega\,(\%)$	$\gamma_{radiative}/\omega\,(\%)$	$\gamma_\alpha/\omega\,(\%)$	$\gamma_{NBI}/\omega\,(\%)$	$\gamma_\sum/\omega\,(\%)$
11	2.12	84.5	-2.15	-0.03	-0.05	-4.49	1.93	10.1	5.3
2	6.7	149.8	-0.18	-0.1	0	0	-0.15	0.76	0.33

Table V: *Growth and damping rates calculation for $n = 11$ TAE and $n = 2$ EAE in a strongly reversed shear ITER plasma. In the table various contributions to the growth rates are presented, such as γ_{iL} ion Landau damping, γ_e electron Landau and collisional damping, $\gamma_{continuum}$ continuum damping, $\gamma_{radiative}$ radiative damping, γ_α alpha particle drive, γ_{NBI} beam ion drive, and total growth rate $\gamma_\sum$ normalized to the mode frequency.*

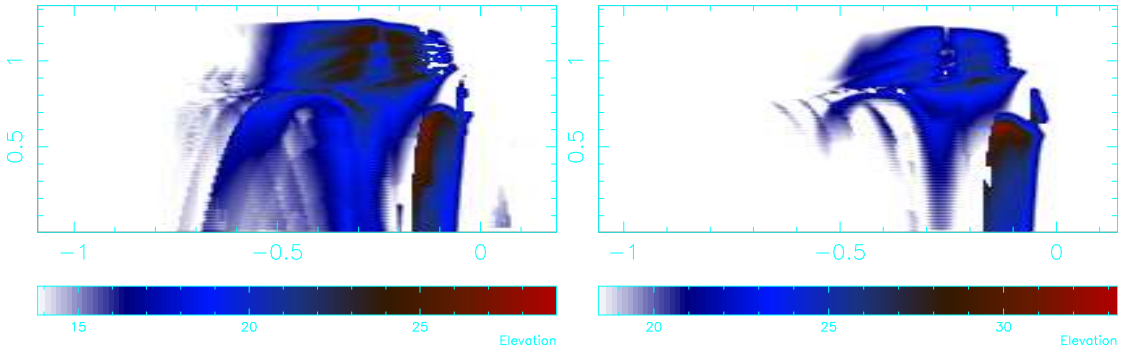

Figure 30: *Relative contributions to the growth rates of the most unstable $n = 11$ TAE in AT plasma shown in Fig. 29 from alphas (left figure) and NNBI confined ions (right figure). Plotted are contours of the logarithm of $\partial^2\gamma/\partial P_\varphi \partial\lambda$ in arbitrary units.*

VII. SUMMARY AND DISCUSSION

In the course of the milestone work we performed a systematic study of three fiducial ITER scenarios: the elmy H-mode, hybrid and advanced (AT or reversed shear) plasma regimes. The TSC and the plasma transport simulation code, TRANSP, were used to model plasmas of these scenarios. Overall, ten additional plasmas, with varying NNBI injection angle and current drive schemes, were developed for the elmy H-mode, hybrid and AT scenarios. This enables an evaluation of the potential of controlling the excitation of fast ion driven TAE (Toroidicity - induced Alfvén Eigenmode) instabilities by varying the injection angle and controlling the safety factor profile.

The stability of Alfvén Eigenmodes with frequencies up to TAE and EAE gap frequencies was simulated numerically with n ranging from 1 to 20, which exceeds the planned value, n=15. Hybrid MHD/kinetic code NOVA-K was applied. In normal shear safety factor plasmas and in hybrid plasmas the NBI injection angle was varied in order to investigate the possibility of TAE stability control. In both scenarios we found the expected medium to high-n range of TAEs unstable when the NBI was aimed slightly off axis, $10-20cm$ vertically away from the midplane. On-axis heating was marginally unstable due to strong central ion Landau damping.

Three ITER AT plasmas were modeled with different values of the shear reversal, which was changing from being close to the hybrid to well reversed. We have found that the plasma in the most reversed shear configuration is the most unstable. This is due to a much wider TAE gap in the strongly reversed case and generally localized solutions near the point of q_{min}, which is close to the maximum gradients of alpha and beam ion pressures. In addition Eq.(1) implies that since the most unstable toroidal mode number depends on the safety factor value, in elmy H-mode and in hybrid scenario unstable ns are similar, whereas in the advanced scenario with $q_{min} \sim 2$ the most unstable mode number is typically lower.

Overall AT and hybrid plasmas are most unstable with the damping rates for the unstable modes approaching $3-5\%$. For the comparison in the elmy H-mode plasma TAE growth rates were within $1-3\%$. Most of the unstable modes in H-mode and hybrid plasmas are localized. One remarkable and dangerous property of the TAEs in AT plasma is that there are much more unstable modes (with most of them weakly unstable, but global), which can result in the multiple mode induced transport of fast ions in ITER.

Another important result is that we identified the most important damping mechanisms. One of them is the ion Landau damping on thermal ions, especially for core localized modes. For the edge localized and global TAEs, electron collisional damping dominates. At high-n numbers radiative damping limits the unstable modes. Continuum damping is important, but in the NOVA model it is not a function of the mode number. It can be often avoided if the mode structure is localized away from the continuum, such as in the cases shown in Figure 21. At high-n limit radiative damping becomes important and contributes to limit the unstable range of TAE mode numbers.

Acknowledgments

In preparation for these milestone activities we greatly benefited from discussions with Drs. E.D. Fredrickson, G.-Y. Fu, R. White, J. Snipes, W.W. Heidbrink, L. Chen, V. Mukhovatov. This work was supported in part by the United States Department of Energy under Contracts No. DE-AC02-76CH03073 and DE-FG03-96ER-54346.

[1] S. C. Jardin, N. Pomphrey, and J. J. Delucia, J. Comput. Phys. **46**, 481 (1986).
[2] R. V. Budny, Nucl. Fusion **42**, 1383 (2002).
[3] C. Z. Cheng and M. S. Chance, Phys. Fluids **29**, 3695 (1986).
[4] G. Y. Fu and J. W. V. Dam, Phys. Fluids B **1**, 1949 (1989).
[5] C. Z. Cheng, Phys. Reports **211**, 1 (1992).
[6] N. N. Gorelenkov, H. L. Berk, and R. V. Budny, Nucl. Fusion **45**, 226 (2005).
[7] N. N. Gorelenkov, H. L. Berk, R. V. Budny, C. Z. Cheng, G. Y. Fu, W. W. Heidbrink, G. J. Kramer, D. Meade, and R. Nazikian, Nucl. Fusion **43**, 594 (2003).
[8] G. Y. Fu, C. Z. Cheng, and K. L. Wong, Phys. Fluids B **5**, 4040 (1993).
[9] G. Y. Fu, C. Z. Cheng, R. Budny, Z. Chang, D. S. Darrow, E. Fredrickson, E. Mazzucato, R. Nazikian, K. L. Wong, and S. Zweben, Phys. Plasmas **3**, 4036 (1996).
[10] N. N. Gorelenkov, Phys. Rev. Letters **95**, 265003 (2005).
[11] N. N. Gorelenkov, C. Z. Cheng, and G. Y. Fu, Phys. Plasmas **6**, 2802 (1999).
[12] D. J. Campbell, Phys. Plasmas **8**, 2041 (2001).
[13] D. Campbell, F. D. Marco, G. Giruzzi, G. Hoang, L. D. Horton, G. Janeschitz, J. Johner, and et. al., in *Proceedings of 21th IAEA Fusion Energy Conference*, Chengdu, China) **IAEA-CN-149-FT/1-1**, 1 (2006).
[14] O. Gruber, J. Hobirk, C. F. Maggi, and et al., Plasma Phys. Contr. Fusion **47**, B135 (2005).
[15] E. Joffrin, A. C. C. Sips, J. F. Artaud, and et. al., Nucl. Fusion **45**, 626 (2005).
[16] M. R. Wade, T. C. Luce, P. A. Politzer, and et al., Phys. Plasmas **8**, 2208 (2001).
[17] R. E. Waltz, G. M. Staebler, W. Dorland, and et al., Phys. Plasmas **4**, 2482 (1997).
[18] P. Strand, H. Nordman, J. Weiland, and J. P. Christiansen, Nucl. Fusion **38**, 545 (1998).
[19] A. Pankin, D. McCune, R. Andre, and et.al., Comp. Phys. Communications **159**, 157 (2004).
[20] M. Brambilla, Plasma Phys. Contr. Fusion **41**, 1 (1999).
[21] M. Evrard, J. Ongena, and D. van Eester, in *AIP Conference Proceedings 335, Radio-Frequency Power in Plasmas, 11th topical conference*, Palm Springs **335**, 235 (1995).
[22] R. V. Budny and C. E. Kessel, to be submitted (2007).

[23] R. B. White, *The Theory of Toroidally Confined Plasmas* (Imperial College Press, London, UK, 2001), 2nd ed.

The Princeton Plasma Physics Laboratory is operated
by Princeton University under contract
with the U.S. Department of Energy.

Information Services
Princeton Plasma Physics Laboratory
P.O. Box 451
Princeton, NJ 08543

Phone: 609-243-2750
Fax: 609-243-2751
e-mail: pppl_info@pppl.gov
Internet Address: http://www.pppl.gov